High energy femtosecond fiber laser at 1018 nm and high power Cherenkov radiation generation

by

Hongyu Yang

B.S., Peking University (2012)

Submitted to the Department of Electrical Engineering and Computer Science in partial fulfillment of the requirements for the degree of

Master of Science in Electrical Engineering and Computer Science

at the

MASSACHUSETTS INSTITUTE OF TECHNOLOGY

September 2014

Signature of Author: Signature redacted

Department of Electrical Engineering
August 29, 2014

Certified by Signature redacted

Franz.X.Kärtner
Adjunct Professor of Electrical Engineering
Thesis Supervisor

Certified by Signature redacted

Erich. P. Ippen
Elihu Thomson Professor of Electrical Engineering and Professor of Physics, Emeritus
Thesis Co-advisor

Accepted by Signature redacted

Leslie A. Kolodziejski
Chairman, Department Committee on Graduate Theses

High energy femtosecond fiber laser at 1018 nm and high power Cherenkov radiation generation

by

Hongyu Yang

Submitted to the Department of Electrical Engineering and Computer Science on

August 29, 2014,

in partial fulfillment of the requirements for the degree of

Master of Science in Electrical Engineering and Computer Science

Abstract

Two novel laser systems for ultrafast applications have been designed and built. For the seeding of a high energy cryogenically cooled Yb:YLF laser, a novel 1018 nm fiber laser system is demonstrated. It produces >35 nJ pulse energy and 5 nm spectral bandwidth. A double-cladd amplifier and an appropriate filter to optimize the system for the amplifier seeding application were employed. This is the highest pulse energy with narrow spectrum at 1018 nm. For a photonic analog-to-digital conversion system operating at 1250 nm, a fiber laser system generating 4 W of femtosecond Cherenkov radiation at that wavelength was built. The characteristics of the Cherenkov radiation were well studied.

Thesis Supervisor: Franz X. Kärtner
Title: Adjunct Professor of Electrical Engineering

Thesis Supervisor: Erich P. Ippen
Title: Elihu Thomson Professor of Electrical Engineering and Professor of Physics, Emeritus

Acknowledgments

Foremost, I would like to express my deepest gratitude to my advisor Prof. Franz Kärtner for his continual support for my master research and study. His inspiring words drive me to achieve a higher level in life and research work. I would also like to thank Prof. Erich Ippen, for his always persistent kindness and encouragement.

I would like to express my gratitude to all those who helped me work and learn since I came into MIT. I am very grateful for the guidance and knowledge that Guoqing (Noah) Chang has given me during my entire study in this group. His support and sparkling ideas always lead me to making progress in the research. I am also thankful to Ronny Huang, who as a close friend and helpful colleague has given me a lot of advice on life and experiment. I am obliged to Hung-Wen Chen and Jinkang Lim who helped me when I ran into many different problems in the lab. I am also thankful to Duo Li, who as a friend and warmhearted colleague shared with me a lot of life and research experience. I am also thankful to Koustuban Ravi, who helped me learn both in science and life. I am thankful for the leadership of research scientists Kyunghan Hong, Luis Zapata, and Jeffrey Moses. I am also thankful for the consistent support that Sergio Carbajo, Emilio Nanni, Peter Krogen, Billy Putnam, Damian Schimpf, Liang jie Wong, and Patrick Callahan have given me in my research and study. Finally, I thank the other staff, postdoctoral colleagues including Yue Zhou, Hua Lin, and Dorothy Fleischer, who have made my life in MIT smooth and happy in their ways.

Finally, I would like to thank my family for their endless support through my studies.

Table of Contents

List of Tables

List of Figures

Chapter 1

Introduction

Lasers have transformed the world since the first working laser was developed in 1960. Fiber lasers were invented in 1961 by Elias Snitzer and his colleagues. Fiber lasers have the advantage of robustness, low-cost, portability, excellent beam quality and insensitivity to thermal problems. In this chapter, we introduce the basic knowledge of the all-normal dispersion (ANDi) fiber laser and Cherenkov radiation.

1.1 ANDi fiber laser

Before the ANDi fiber laser was invented, most femtosecond fiber lasers need a dispersion compensation device like a prism [1], diffraction gratings [2], or chirped mirrors [3] to form an anomalous dispersion in the cavity, which along with the balance of the fiber nonlinearity constitutes a pulse-shaping mechanism. In recent decades, with the development of in-line components like photonic-crystal fiber (PCF) and hollow-core fiber [4-6], anomalous dispersion in single fiber becomes possible. In 2004, Buckley *et al.* theoretically showed that a frequency filter helps stabilize the mode-locking operation in a cavity with anomalous group velocity dispersion (GVD) [7]. It also introduces self-phase modulation to allow nonlinear-polarization evolution to work as a fast saturable absorber in the laser cavity. However, in Buckley *et al.* 's work, an additional grating pair is still needed to ensure the mode-locking. Andy Chong *et al.*, in 2006, built a laser cavity using only normal-dispersion elements and generated ~100 fs pulses [8]. This concept gives rise to the compact portable femtosecond laser sources, noticeably reducing the size and cost of a femtosecond laser.

1.1.1 Mathematical description of theANDi fiber laser

The mathematical description of the pulse shaping in an ANDi fiber laser is given in the following equation [9]:

$$\frac{\partial A(z,\tau)}{\partial z} + i\frac{\beta_2}{2}\frac{\partial^2 A(z,\tau)}{\partial \tau^2} = i\gamma\left|A(z,\tau)\right|^2 A(z,\tau) + g(E_{pulse})A(z,\tau)$$

where $A(z,\tau)$ is the envelope of the field, z the propagation distance and τ the pulse local time. The pulse energy is given by

$$E_{pulse} = \int_{-T_R/2}^{T_R/2} \left|A(z,\tau)\right|^2 d\tau$$

where T_R is the cavity round-trip time. Typical parameters can be found in reference [8]. The split-step Fourier transform method is used to incorporate the nonlinear effects and dispersion effects.

1.1.2 Properties of the ANDi fiber laser

An ANDi laser has many advantages over traditional fiber lasers. First, it has no costly and bulky anomalous-dispersion elements, making all-fiber laser design much easier. Second, it can bear a larger nonlinear phase shift inside the cavity, around 16π, so that higher pulse energy can be obtained from the cavity. In contrast, the largest bearable nonlinear phase shift in a soliton fiber laser (or stretch-pulse fiber laser), is only ~0.1π (or ~π) [9]. Third, the spectrum is tunable within a certain range, making the laser versatile.

ANDi lasers have other unique features that make them useful in many applications. First, the output spectrum looks like a transmission curve of a notch-filter. This is due to the narrow band-pass filter used in the cavity to cut off the spectrum and also the pedestal of the pulses. Second, the pulse energy is an order of magnitude higher than the pulse energy from the stretch-pulse fiber lasers, and two order of magnitude high than that in a soliton mode-locked fiber laser. Third, given no fundamental environmental change, the pulse is always self-sustained and self-starting. Stable mode-locking operation can be kept for weeks in the lab environment. Fourth, the pulse duration increases almost linearly along the cavity, and only sharply decreases at the saturable absorbers.

1.2 Fiber-optic Cherenkov radiation

Fiber-optic Cherenkov radiation (FOCR), also known as dispersive wave generation or Vavilov-Cherenkov radiation, is radiation from a soliton pulse propagating in an optical fiber that is perturbed by high-order dispersion [10-14]. It is used primarily as a wavelength conversion technique for generating isolated spectra in the visible wavelength range. With the development of photonic-crystal fibers (PCFs), FOCR has attracted more research interest [15-25]. In 2005, Fei Lu and Wayne Knox studied the FOCR and four-wave mixing using millimeter-scale dispersion management technique in holey fibers [26]. The longitudinal properties of FOCR generation were studied and used to generate broad bandwidth. G. Chang *et al.* recently introduced the coherence length to quantify the behavior of FOCR generation, and studied the FOCR in the few-cycle regime for visible wavelength generation with high efficiency both theoretically and experimentally [27]. Chris Xu's group recently has demonstrated generation of Cherenkov radiation in high-order mode (HOM) fiber using a commercial femtosecond fiber laser with a few nJ of pulse energy [28]. Further efficient femtosecond Cherenkov radiation generation in his recent work showed conversion efficiency about 20% and a pulse duration as short as 134 fs [29].

1.2.1 Mathematical description of Cherenkov radiation

The mathematical description for the ultrashort pulse propagation is given in the generalized nonlinear Schrödinger equation (GNLS):

$$\frac{\partial A}{\partial z}+\left(\sum_{n=2}^{\infty}\beta_n\frac{i^{n-1}}{n!}\frac{\partial^n}{\partial T^n}\right)A=i\gamma\left(1+\frac{i}{\omega_0}\frac{\partial}{\partial T}\right)\left(A(z,T)\int R(t')\left|A(z,T-t)\right|^2dt'\right)$$

where $A(z,t)$ is the envelop of the field, β_n the nth order dispersion valued at the central wavelength ω_0, and γ the nonlinear parameter of the fiber. R(t) describes the behavior of the instantaneous scattered Raman-soliton in the fiber.

$$R(t) = (1 - f_R)\delta(t) + f_R[(f_c + f_a)h_a(t) + f_b h_b(t)]$$

Typical parameters can be found in the ref. [18].

The phase matching condition of $\Delta\beta = 0$ for the FOCR generation is given in the following equation [26]:

$$\Delta\beta = \beta(\omega) - \beta(\omega_s) - \frac{\omega - \omega_s}{v_g} - \gamma P_s$$

where β is the propagation constant. ω_s and ω are the soliton and Cherenkov radiation frequencies, respectively. v_g is the group velocity, γ the fiber nonlinear coefficient, and P_s the soliton peak power.

A coherence length was also introduced to describe the phase-mismatch that causes a spectral narrowing effect:

$$L_c(\omega) = \frac{\pi}{|\Delta\beta(\omega)|} = \frac{\pi}{\left|\sum_{n=1}^{\infty} \frac{(\omega - \omega_s)^n}{n!}\beta_n(\omega_0) - \frac{\gamma P_0}{2}\right|}$$

where the symbols have the same meanings as before.

1.2.2 Properties of Cherenkov radiation

Theoretical study of FOCR using numerical method was carried out in Ref. [26, 27]. At its initial buildup, the Cherenkov radiation is much weaker than the soliton. As it evolves along the fiber, quadratic growth of power will occur. The spectrum of FOCR is often limited due to the large frequency separation between the FOCR and its pump soliton. In terms of coherence length, when the distance between the FOCR and the pump soliton is L_c, a destructive inference occurs and dampens the rapid power buildup process.

1.3 Organization of the thesis

The rest of this thesis is organized as follows:

Chapter 2 describes the idea of building an ANDi laser system at 1018 nm with tens of nJ pulse energy for seeding Yb:YLF amplifier . The motivation for this oscillator is discussed. Some simulation method and results are provided for better understanding of the fiber laser characteristics. The experimental design and results are also given in the context. Simulation for the oscillator is also discussed in detail.

Chapter 3 describes the idea of using a 3 GHz high power laser and a dispersion compensation device to generate high power Cherenkov radiation pulses. Experimental results showed a record high efficiency for generating Cherenkov radiation. This Cherenkov radiation has pulse duration in the picosecond and sub-picosecond regime.

Appendix A gives a list of components for re-producing a 1018 nm fiber laser system. Specifications of some components are also provided.

Appendix B provides a sample MATLAB code for simulation the 1018 nm fiber laser system. This code can be adapted for simulating other pulsed fiber laser systems.

Chapter 2

High energy 1018 nm femtosecond fiber laser system

This chapter describes an Yb-fiber laser system generating stable 1018 nm narrow bandwidth femtosecond pulses with >35 nJ pulse energy. This is by far the highest pulse energy with compressible pulses at 1018 nm generated from an ANDi fiber laser. By suppressing the thermal issue around the splicing point in the power amplifier, pulses with energy over 100 nJ should be possible.

2.1 Introduction and motivation

High energy and high power has been a focus of pulsed laser systems for decades. The ytterbium laser has been widely studied in the past decades because of its high optical-to-optical efficiency for generating high power and high energy pulses. To achieve tens of microjoule level pulse energy at 1 μm, regenerative amplifiers have to be used to accommodate the nonlinearity during the amplification stage. Among ytterbium doped materials, Yb:YLF crystals have many advantages such as wide spectral emission range [30], low nonlinearity and high thermal conductivity; they can generate over 30 mJ energy femtosecond pulses at tens of Hertz rates and have the potential tor increasing the repetition rate to kilo-Hertz rates if a thin-disk laser is used to help remove the thermal issue [31]. A good fiber-based seed laser will facilitate the regenerative amplification, suppressing the amplified spontaneous emission (ASE) and incorporating the advantage of low-cost and compactness of the fiber. However, Yb:YLF regenerative amplifiers have a very narrow gain bandwidth of about 5 nm around 1018 nm, which is at the low-gain region of the ASE. Little work in the past has been devoted specifically to 1018 nm femtosecond fiber lasers. Research has been focused on 1018 nm high power continuous-wave lasers [32, 33]. Yb-doped phosphosilicate fiber and Yb-Doped double-clad fiber were used in both oscillator and amplifier to generate a 1018 nm centered spectrum. A high energy pulsed ytterbium fiber laser operating at 1018 nm has not been reported. Here we demonstrate a 1018 nm femtosecond ANDi fiber laser with over 35 nJ pulse energy and a spectrum matching the emission spectrum of Yb:YLF materials.

2.2 Limitation and design

While a fiber laser is promising for making high energy 1018 nm seed oscillator, it has some intrinsic limitations.

The first limitation comes from the special wavelength. The gain bandwidth of the Yb:YLF is only around 5 nm around 1018 nm. This is not at the peak of the regular emission curve of the Yb-doped fiber, which is shown below in Fig.2.1. Typically pumped at 975 nm, the highest gain is at 1031 nm. Due to the broad gain bandwidth of Yb-doped fiber, the ASE amplification and the energy-shifting to longer wavelength will suppress the amplification of the signal if the incoming signal at 1018 nm is not strong enough. It may also cause parasitic lasing [32]. To avoid these issues, some high-efficiency CW lasers and amplifiers at 1018 nm were designed [32, 33]. We choose a special doped double-clad Yb-fiber that has a flattened absorption but a smaller peak at 1018 nm on its emission curve, which corresponds to the green and purple curves shown in Fig.2.2. This Yb-fiber has a similar emission cross section to that of the Yb-doped phosphosilicate fiber used in Ref. [32], but also preserves the convenience of easy splicing and strong cladding-pumping, making it promising for building a 1018 nm fiber amplifier.

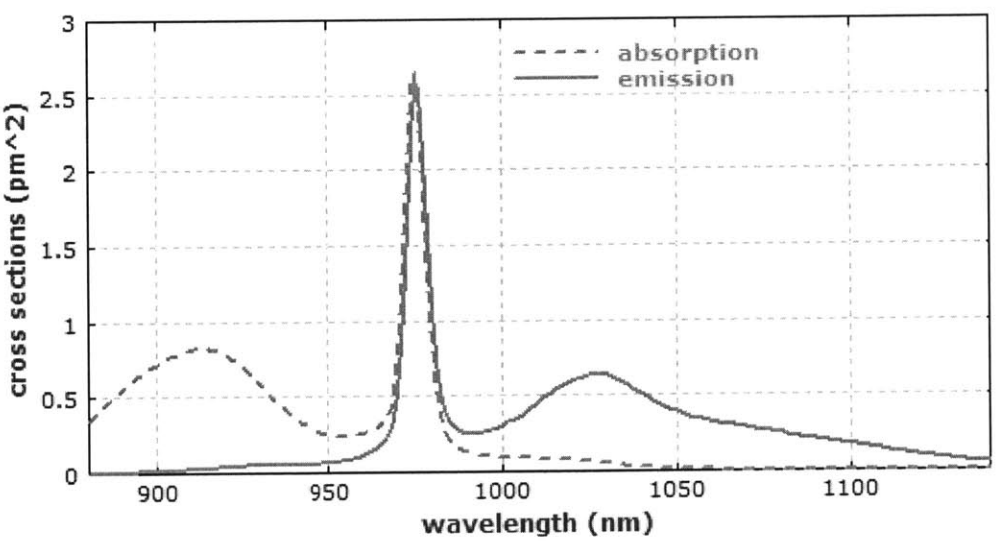

Fig.2.1: Absorption and emission cross section of yitterbium-doped germanosilicatesglass. (source: http://www.rp-photonics.com/ytterbium_doped_gain_media.html)

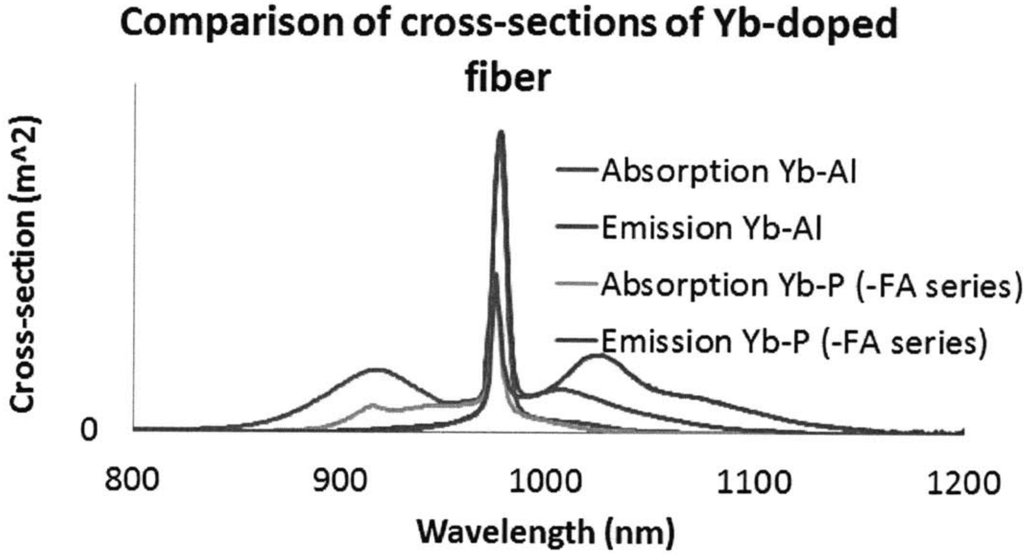

Fig.2.2: Absorption and emission cross section of different Yb-doped fiber.
(source: www.coractive.com)

Another limitation is on the repetition rate. With limited pump resource, the amplified power for a femtosecond pulse train is typically restricted to hundreds of milliwatts for a single-mode amplifier, a few hundreds of watts for a double-clad fiber amplifier, and a few hundred watts for a rod-type fiber amplifier. For the purposes of generating high pulse energy, and saving the cost of expensive pulse-pickers and amplifier stages, people want to have a seed fiber laser with the lowest achievable repetition rate. However, the repetition rate has never been achieved close enough to the damage threshold (about 5 W/μm^2) of the fiber amplifier. Significant work has been done on achieving a repetition rate less than 10 MHz [34-43]. But there is some limitation on the lowest repetition for fiber lasers. Around year 2000, most relative stable fiber lasers had repetition rates higher than 20MHz and less than 100 MHz [34]. In Ref. [34], mode-locking was studied at 10, 15, 20, and 30 MHz. For repetition rate below 20 MHz, very careful adjustment of the waveplates was needed to mode-lock the laser, and it frequently jumped into the multi-pulsing regime. In Ref. [35], W.

H. Renninger *et al.* successfully amplified 3 MHz pulses with giant chirp and compressed them to 670 fs. In 2006, S. Zhou *et al.* designed a hybrid cavity that employs both a single-wall carbon nanotube saturable absorber and the NPR mechanism to mode-lock the laser [36]. However, the pulse energy was only 0.23 nJ. With the development of robust SESAMs (semi-conductor saturable absorber mirrors) [37] and chirped mirrors [38], and the demand for micro-joule level fiber laser systems, several other schemes [39-42] have been proposed, using multi-path cavities (MPC) or long fibers, for building a long cavity. But either the pulses were stretched to the nano-second level and the researchers were not able to compress them back to the femtosecond regime, or the bandwidth of the spectra were limited by the saturable absorber. In 2009, H. Sayinc *et al.* demonstrated that a 1.8 MHz fiber laser system can have both stability and compressible pulses (93 fs) using both SESAM and NPR techniques [43].

The highest pulse energy allowed in the oscillator is typically less than 1 nJ for soliton mode-locked lasers, a few nJ for stretched-pulse mode-locked lasers, and 20 nJ for ANDi fiber lasers because of the maximum nonlinear phase shift they can tolerate inside their cavities [44].

For our application, the laser should have a relatively low repetition rate so that fewer amplifier stages are needed, and should preserve high pulse energy in the suitable wavelength range for seeding the regenerative amplifier. To this end, we chose to build an ANDi fiber laser with repetition rate about 13 MHz.

2.3 Simulation

A block diagram of an ANDi fiber laser is shown below for simulation.

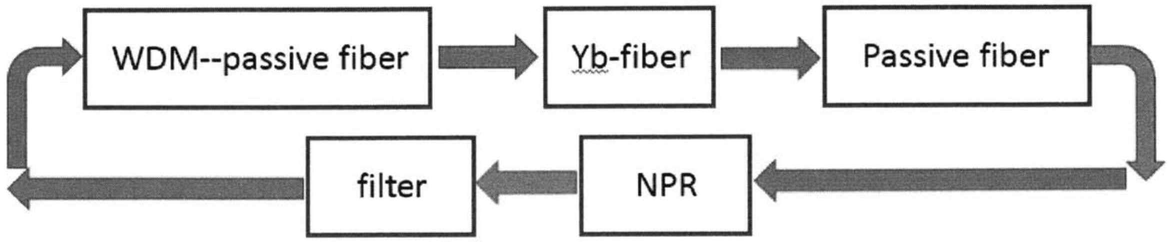

Fig.2.3. Block diagram of the ANDi fiber laser for simulation.

When the pulse is propagating through the fiber, the nonlinear effect and dispersion effect will make changes to the pulse. While they in fact act simultaneously, we treat them separately in simulation using a split-step Fourier Transform method. Several reference papers [45-48] suggest the typical values of the parameters for our simulation:

For passive HI1060 fiber, β_2 = 22.0 fs^2, β_3 = 74.0 fs^3, n_2 = 2.36e-20 m^2/W, A_{eff} = 28.27 μm^2, $\gamma = \frac{2\pi}{\lambda * n_2 * A_{eff}}$, $L_{NL} = \frac{1}{P*\gamma}$, $E_{saturation}$ = inf, g2= 5000 nm. For Yb-4/1200 fiber, β_2 = 23.0 fs^2, β_3 = 74.0 fs^3, n_2 = 2.36e-20 m^2/W, A_{eff} = 15.20 μm^2, $\gamma = \frac{2\pi}{\lambda * n_2 * A_{eff}}$, $L_{NL} = \frac{1}{P*\gamma}$, $E_{saturation}$=3~16, g2 = 350 nm. Here β_2 is the second-order dispersion, β_3 the third-order dispersion, n_2 the nonlinear coefficients, A_{eff} the effective mode-area, $E_{saturation}$ the saturation level, reflecting the pump power and adjustable, L_{NL} the nonlinear length, and g2 the gain-bandwidth.

For the NPR, we model it as a fast saturable absorber, and the saturation depth and response time are adjustable. 70% of the power was coupled out from the cavity. The filter is modeled in the frequency domain.

The real code contains both Visual Fortran and Matlab software. A pseudo code flow of the simulation is in the box below:

```
Program main
{
        set parameters:
                fiber lengths, dispersion, nonlinear coefficients, Raman-coefficients,

        For each roundtrip
        {
                If not converged then
                        Call Progagation(first segment of fiber)
                        Call Progagation(second segment of fiber)
                        Call Progagation(in third segment of fiber)
                        Call NPR and OC
                        Call filter
                else break and save the field
                end
        }
}

Function Propagation  // split-step FT
{
        Call dispersionEffect(dz/2)
        Call nonlinearEffect(dz)
        Call dispersionEffect(dz/2)
}
Function dispersionEffect()
{
        ...
}
Function nonlinearEffect()
{
        ...
}
Function NPRs()
{
        ...
}
Function filter()
{
        ...
}
```

Table.2.1 Code flow for simulating the oscillator

Simulation results for a 13 MHz fiber oscillator are shown below in Fig.2.4. From top to bottom are: the output spectrum, the field intensity in time-domain, and the Fourier transform-limited (TL) pulse. Lengths of the fibers were set to 1400 cm, 25 cm, and 50 cm, respectively for the three segments. Esat for the Yb-fiber was set to 4 and the small signal gain was set to 40 dB.

As can be seen, the spectrum is centered at 1018 nm and spans about 6 nm, which is suitable for our application. The direct output pulse duration is about 4 ps, which may need to be stretched further to above 10 ps for the amplifier. The TL pulse duration is about 320 fs.

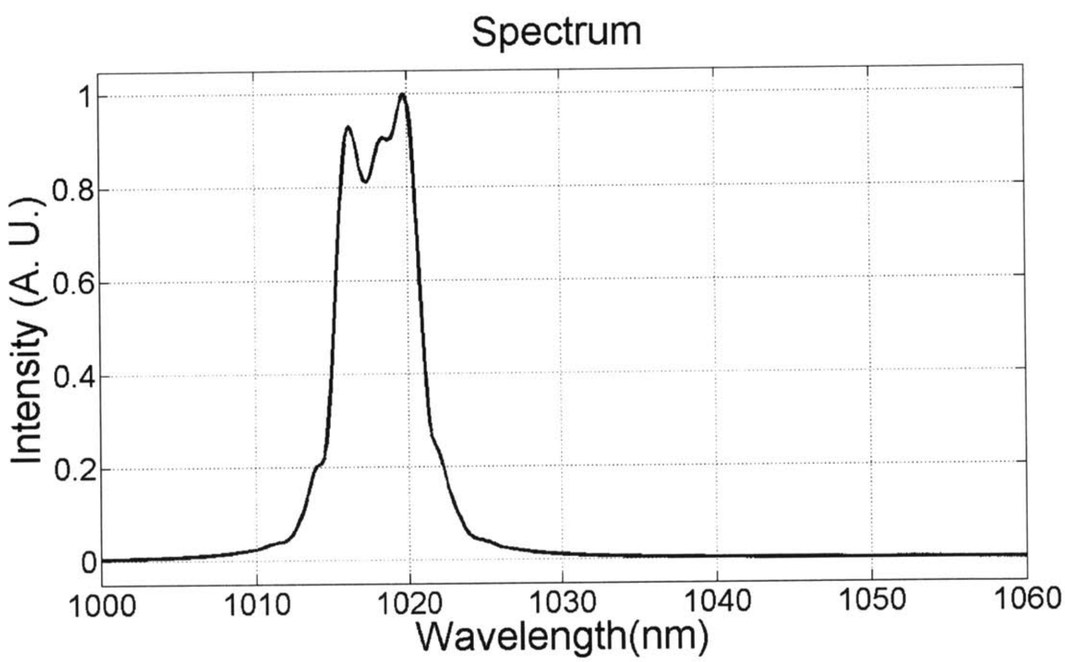

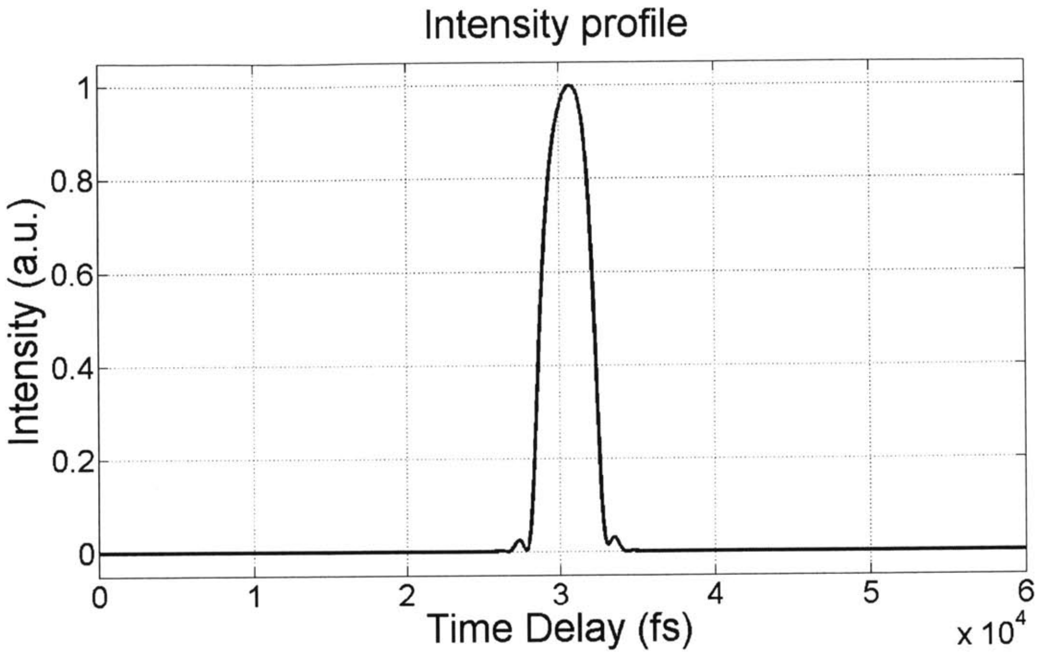

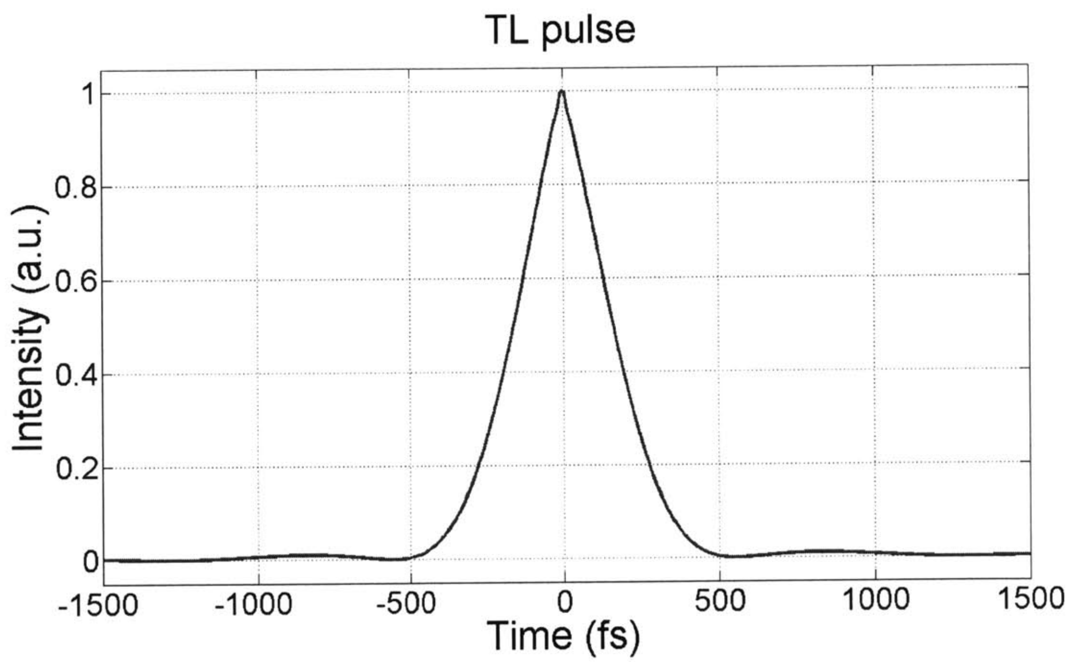

Fig.2.4 Simulation results: (top to bottom) pulse spectrum, pulse intensity in time-domain, and transform-limited pulse

2.4 Experiment setup and results

A schematic diagram of the laser configuration is shown in Fig. 2.5. It consists of an oscillator, a fiber stretcher, a bandpass filter, and a fiber amplifier. The oscillator is an ANDi fiber laser as shown in the block diagram in the previous section, using nonlinear-polarization rotation (NPR) and a spectral filter as the mode-lock mechanisms. The first segment of WDM-isolator fiber is about 1400 cm. The Yb-fiber is 25 cm Yb1200-4/125 highly doped fiber. The third part of the coupler-collimator fiber is about 50 cm. A bandpass filter (BPF) with 3.5 nm bandwidth and flat-top shape (Appendix A.1) was employed to facilitate the mode-locking and tune the center-wavelength of the spectrum so that it covered 1018 nm. Typically, a Gaussian-shaped birefringence filter (Lyot filter) works best for ANDi fiber lasers [49]. However, it needs too many birefringence filters to make a 3-nm-bandwidth filter and adds too many knobs into the cavity. Since the Yb-4/1200 fiber does not have a high gain at 1018 nm, careful adjustment is needed to mode-lock the laser using this 3.5 nm narrow bandpass filter. A 40:60 coupler was used and the 60% portion was coupled out into a fiber-based isolator and then launched into a segment of 20 m long HI-1060 fiber stretcher. Another BPF was employed and tuned between the stretcher and the double-clad amplifier to select the signal wavelength for amplifying and cut unwanted signal spectrum. Leaving out this BFP will make the output spectrum from the amplifier shift to higher wavelength than 1030 nm. The amplifier consists of a (2+1) beam combiner and 50 cm of absorption-flattened Yb-doped double-clad fiber (FP fiber). This kind of FP fiber has a higher gain at 1018 nm than 1030 nm or higher wavelength, enabling efficiently amplifying the signal wavelength. According to the experimental results, either using the filter or the FP gain fiber alone cannot guarantee correct amplification at 1018 nm.

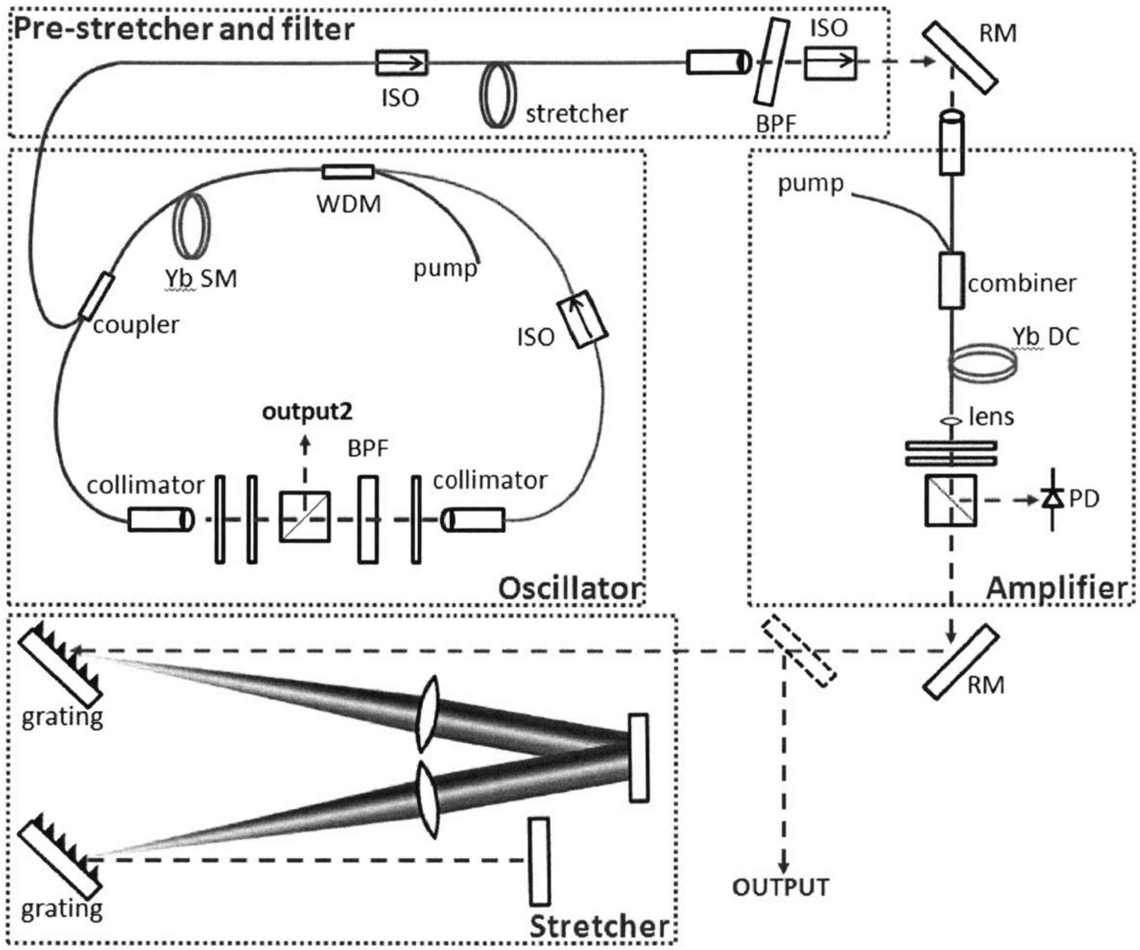

Fig.2.5. Configuration of 1018 nm laser system. ISO: isolator; BPF: band-pass filter; RM: reflecting mirror; PD: photodiode; Yb SM: ytterbium-doped single-mode fiber; Yb DC: ytterbium-doped double-clad fiber.

With the NPR mechanism combined with a spectral filter as the mode-locking mechanism, the seed oscillator worked at repetition rate as low as 12.86 MHz using a 976 nm pump with 300 mW optical power. The spectra of output1 and output2 are shown in Fig.2.6. The output pulse from the coupler in the oscillator has a pulse duration around 3 ps. After the fiber stretcher and band-pass filter, the direct output pulse width was measured to be 4.3 ps (Fig.2.8 inset). With 1W multimode 976 nm optical pumping, 450 mW 1018 nm narrow band output was achieved, corresponding to 35 nJ pulse energy. A pair of diffraction gratings with 600 gr/mm and distance of 30 cm compressed the amplified pulses and the autocorrelation trace of the compressed pulse is 781 femtosecond, as shown in Fig.2.8. The retrieved pulse width is 513 fs. This is within 20% of the transform limited pulse width of the spectrum, confirmed by our simulation results in the previous section. The pulse is relatively clean considering the high pulse energy and short pulse width. The pedestal in the compressed pulse is due to the uncompensated high order dispersion introduced by the grating pair, which can be further compensated by prism pairs with high efficiency.

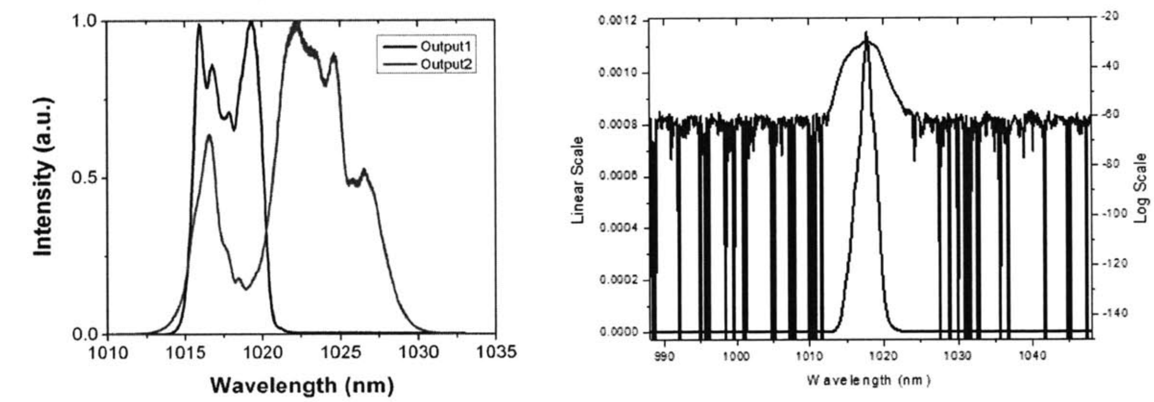

Fig.2.6. left: Output spectra from different ports of the system; right: spectrum after the filter.

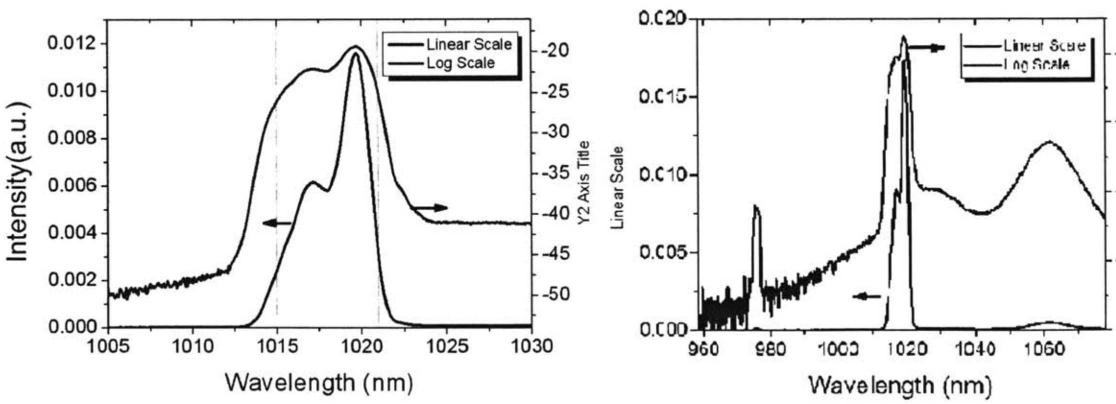

Fig2.7. Output spectrum in narrow (left) and wide (right) wavelength ranges.

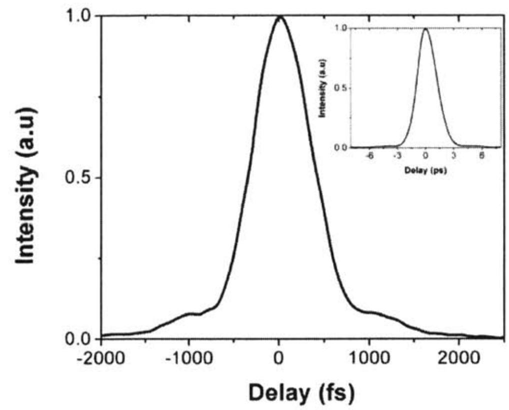

Fig.2.8. Autocorrelation trace of the direct output pulse (inset) and compressed pulse.

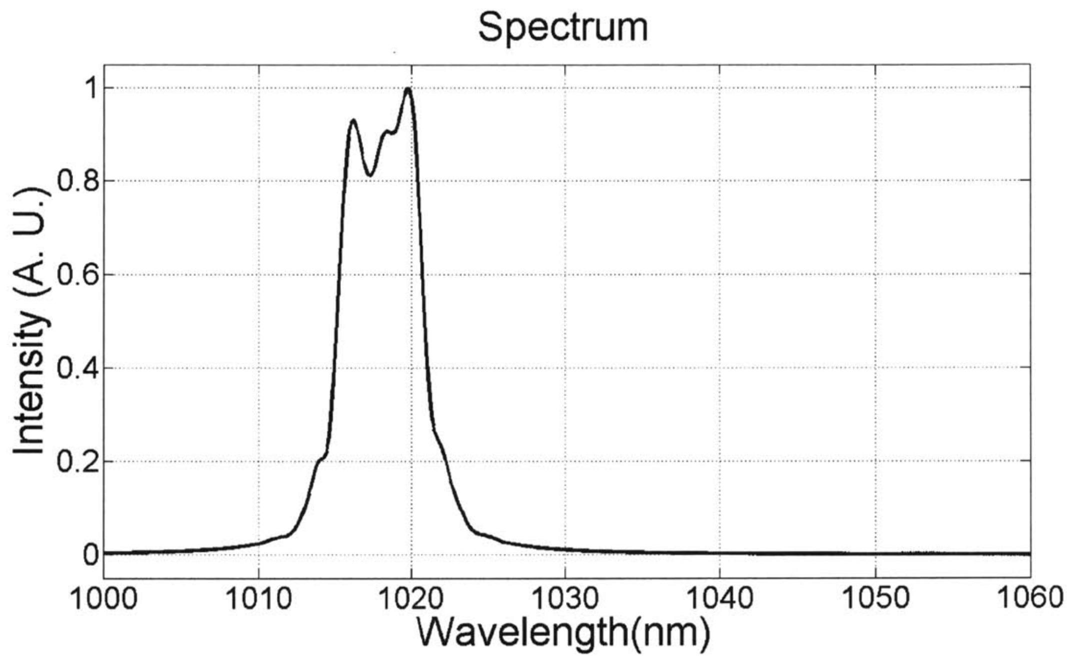

Fig.2.9. Simulated output spectrum of the 1018 nm pulse.

Figure 2.6 shows the oscillator spectrum. This is a typical spectrum of an ANDi fiber laser, with sharp edges on both sides showing the strong effect of the frequency filter. The fringes on the spectrum are a sign of nearly-overdriven nonlinear polarization rotation. Figure 2.7 shows the final output spectrum in linear and logarithmic scales. This is a correct fit for the Yb:YLF regenerative amplifier considering its gain characteristics. The measurement resolution is 0.1 nm.

Figure 2.9 is the simulated spectrum from the oscillator. A Gaussian-shaped filter was assumed and the $1/e^2$ bandwidth was set to 4 nm. Compared to Fig.2.6, we can see, it resembles the real spectrum in the bandwidth and shape. The difference on the top comes from the difference between the real window-like filter and this Gaussian filter in our modeling, and the difference between the gain shape in experiment and in simulation. Simulation suggests that over 200 nJ pulses are possible, but that involves either a CPA system or another double-clad fiber amplifier stage.

Figure 2.10 is a photo showing the whole setup and the compactness (only 60 cm by 60 cm) of this system including all the electronics except the controller of the laser diodes. It makes the laser a great source for many large complex laser systems.

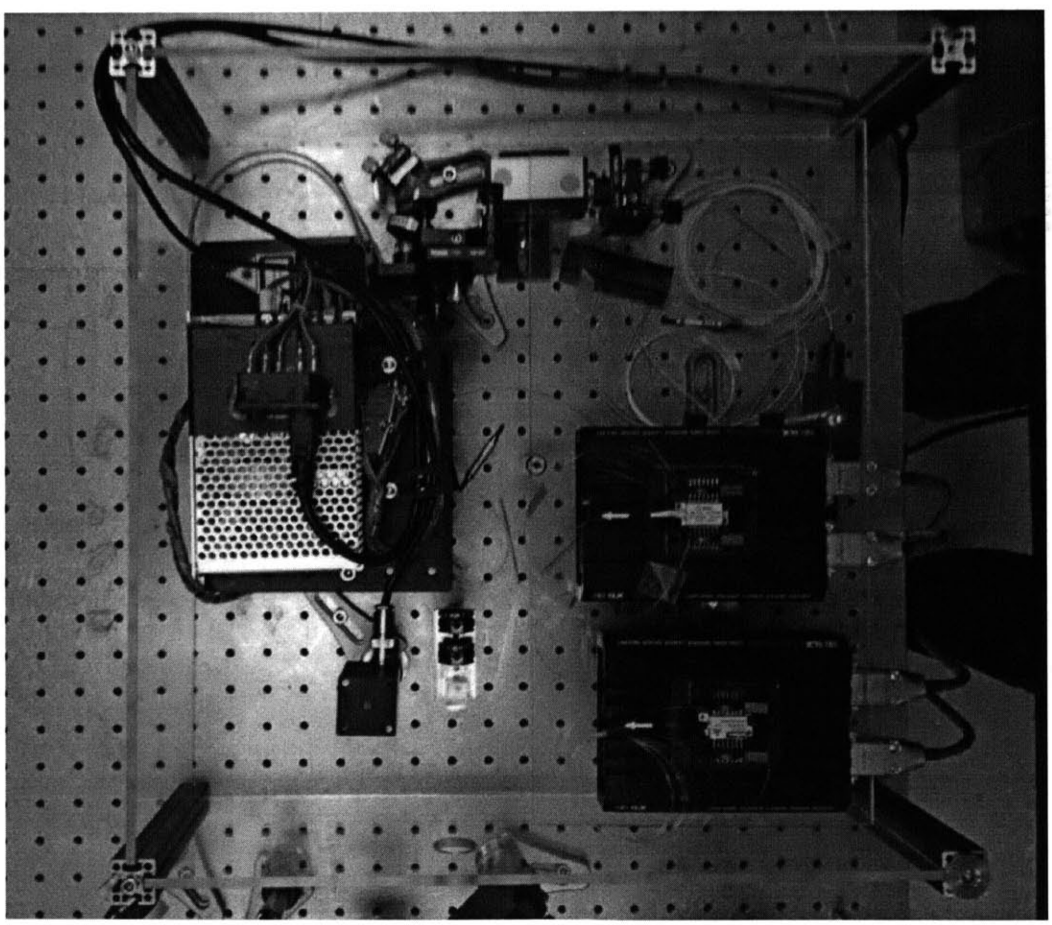

Fig.2.10. A photo of the setup.

Further increasing the pump power for the amplifier simply increases the output pulse energy to the over-100 nJ level. However, no passive fiber should be attached to the double-clad Yb-doped fiber. Otherwise significant nonlinearity will occur and the pulse shape will be distorted. The output was collimated by a free-space collimating lens to avoid this pulse degradation. Mode-locking was stable and self-sustained for a week. However, the repetition rate was somewhat low to maintain a self-starting operation for a long time because accumulated birefringence caused by temperature fluctuation and mechanical perturbation is too high for the nonlinear polarization rotation mechanism to make the mode-locking self-starting in such long fiber in a long run. Further adjustment of the waveplates is needed to restart the mode-locking.

Since the laser is running at a relatively low repetition rate, multi-pulsing can occur if some perturbation happened to the oscillator. That can be mechanical disturbance of the fibers, temperature fluctuation, or acoustic noise induced birefringence change. A typical reflection of those changes is the modulation on the spectrum; an example is given in Fig.2.11 (left). To get a super-stable mode-locking operation, auto-adjustment mechanics and the temperature controller have to be implemented into the system. Another key point is using the narrow bandwidth bandpass filter and the special DCYb-8/125 fiber at the same time. Since the double-clad fiber has relatively low absorption at 975 nm, meters of this gain fiber should be used. On the other hand, the longer the gain fiber, the more energy will be transferred to, and amplified at, longer wavelength. This is because fiber intrinsically has higher absorption at shorter wavelength than longer wavelength. If the seeding signal is weak or has a spectrum residual that is close to 1030 nm, the residual will sees a higher gain. That situation is reflected in Fig.2.11 (right). In summary, the double-clad Yb-doped fiber amplifier tends to have an output at longer wavelength. To get the clean spectrum at the desired wavelength, one or more filters are necessary depending on how much power to expect from the amplifier.

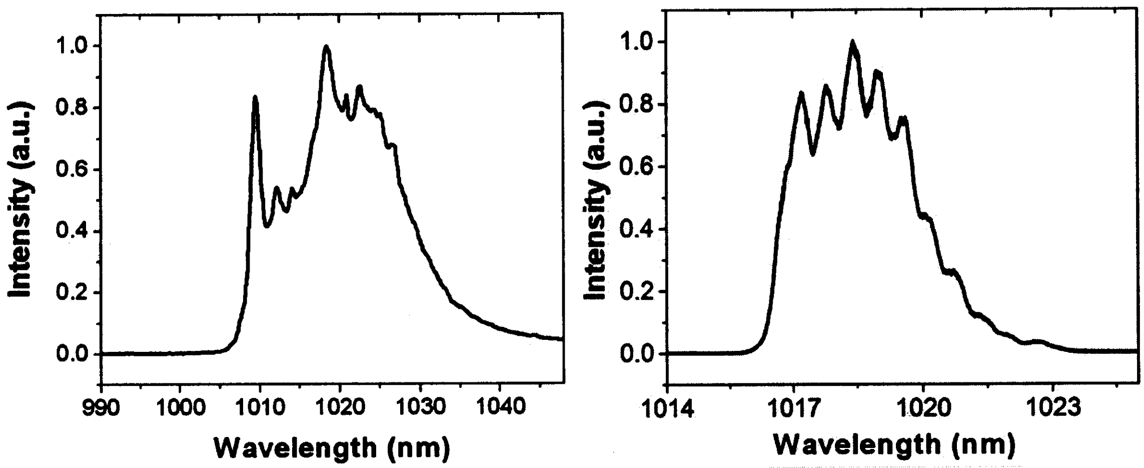

Fig.2.11 left: amplified spectrum with energy shifted to longer wavelength; right: amplified spectrum with modulation.

2.5 Conclusion

In conclusion, we designed, simulated and built the highest energy narrow band 1018 nm femtosecond fiber laser system to date. This laser system is able to deliver over 35 nJ femtosecond pulses with spectral bandwidth about 5 nm. Two spectral filters were used to constrain the seeding spectrum for the amplifier. The pulse duration can be compressed to 513 fs. It is a promising seed laser for a Yb:YLF regenerative amplifier. This system incorporates a low-cost ANDi fiber laser seed, a narrow band filter for selective amplification, and absorption-flatten double-clad Yb fiber for amplification with suppressed ASE, which has the advantage of compactness and easy maintenance.

Chapter 3

High power Cherenkov radiation

In this chapter, we discuss in detail the high power Cherenkov radiation. A novel device with high order mode fiber was employed to provide large anomalous dispersion for Cherenkov radiation generation. 155 fs pulses with 3 GHz repetition rate were achieved with a 2.4W input pulse.

3.1 Introduction and motivation

Femtosecond laser pulses at around 1200nm have many applications in biomedical and bio-imaging area. Over the last few decades, works have been devoted to soliton frequency shift as well as energy transfer to this particular wavelength [50-55]. Because of the lack of anomalous dispersion devices at this wavelength, early laser sources were restricted to wavelengths greater than 1300 nm [50, 51]. With the recent development of photonic-crystal fibers (PCFs), dispersion becomes controllable and tunable sources for a wider wavelength range are available. Unfortunately, the pulse energy required for stable Raman-shifted solitons is on the extreme ends, either just sub-nJ for the PCF or hundreds of nJ for the photonic-crystal bandgap fibers (PBGFs), because of the high nonlinearity of the PCF and the low nonlinearity in the PBGF, respectively [56]. For the purpose of generating Raman-soliton pulses with few nJ pulses, Siddharth Bhardwaj, a fellow graduate student, developed a high order mode fiber that preserve relatively large effective area and large anomalous dispersion around 1200 nm [19]. This facilitates the generation of compressible Raman-soliton pulses but alongside produces nontrivial portion of Cherenkov radiation [57]. Here we use this device to generate compressible Cherenkov radiation with the highest reported optical power.

3.2 System design, experimental results and discussion

To generate the most possible output power, we used the 3 GHz laser system in reference [57]. This system delivers over 3 nJ, 100 fs compressed pulses as excitation pulses for Cherenkov radiation generation. The device is a concatenation of a segment of HI780 fiber, a piece of fiber Bragg-grating, and a segment of high order mode fiber. A schematic of the device is shown below:

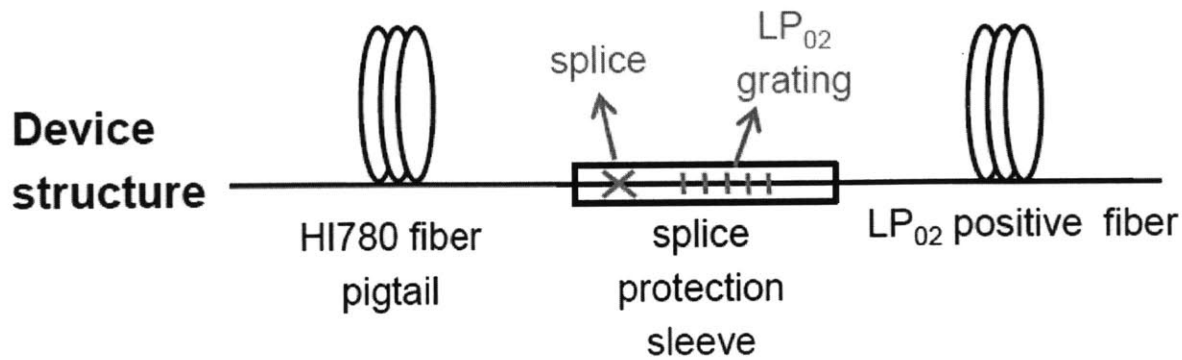

Fig.3.1. Structure of the device.

Only the high order mode of the LP02 positive fiber provides anomalous dispersion for the soliton propagation and Cherenkov radiation generation. Its nominal insertion loss is about 0.5 dB in total for 1 μm pulses. The dispersion curve for the LP02 positive fiber is given below in Fig.3.2. This suggests that in a short segment of fiber we can generate Raman-solitons below 1200 nm and in a long segment, we can produce Cherenkov radiation above 1200 nm.

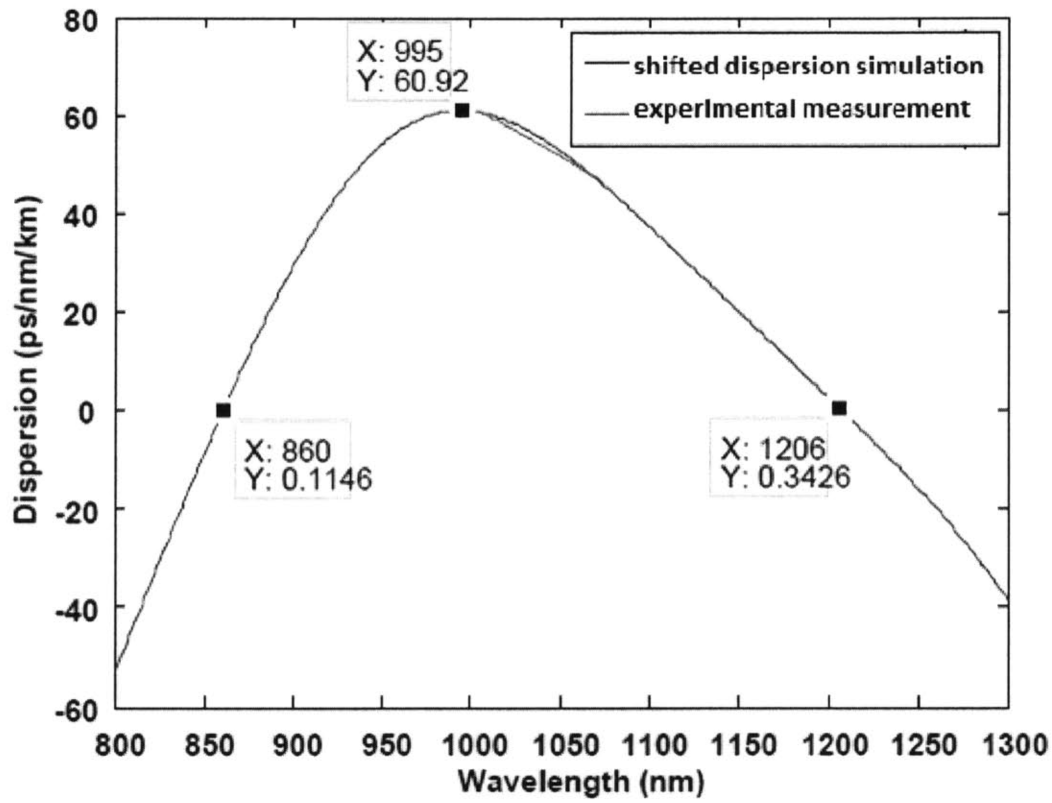

Fig.3.2. Dispersion curve of the LP02 positive fiber with ZDW points indicated.

Simulation suggests that the Cherenkov radiation with maximum power can be obtained with 0.75 m LP02 positive fiber and no HI780 fiber in the front end. This is shown in Fig.3.3. An initial pulse with Gaussian profile and 100 fs pulse duration (FWHM) is assumed.

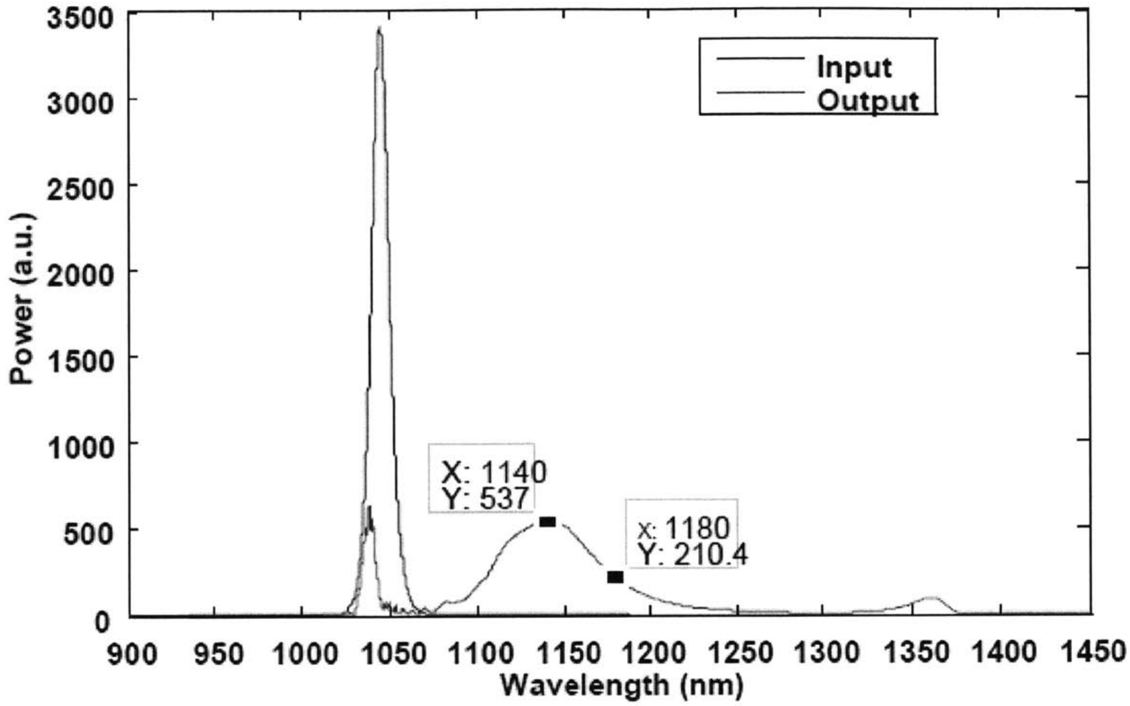

Fig.3.3. Spectra of simulated input host pulse and output frequency-shifted pulse.

The system setup is shown in Fig.3.4. A half-wave plate is placed before the LP02 positive fiber for optimizing the output Cherenkov radiation. A long pass filter after the output lens eliminates the Raman-soliton pulse and the residual host pulse.

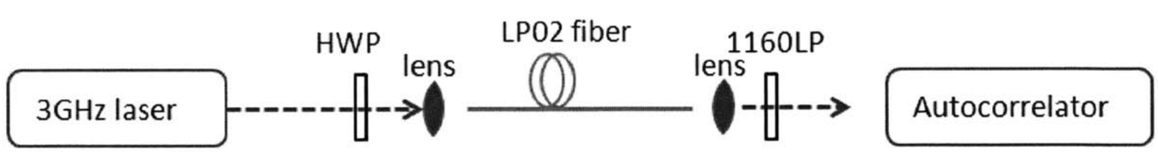

Fig.3.4. Cherenkov radiation system setup: HWP: half-wave plate; 1160LP: 1160 nm long-pass filter.

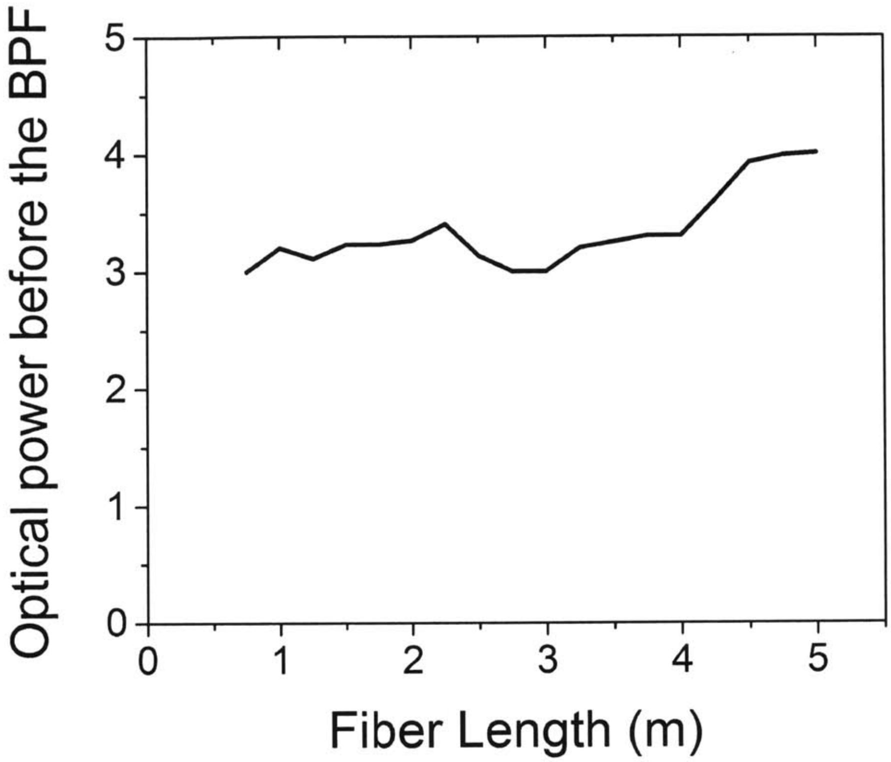

Fig.3.5. Optical power of the frequency-shifted pulse before the band-pass filter.

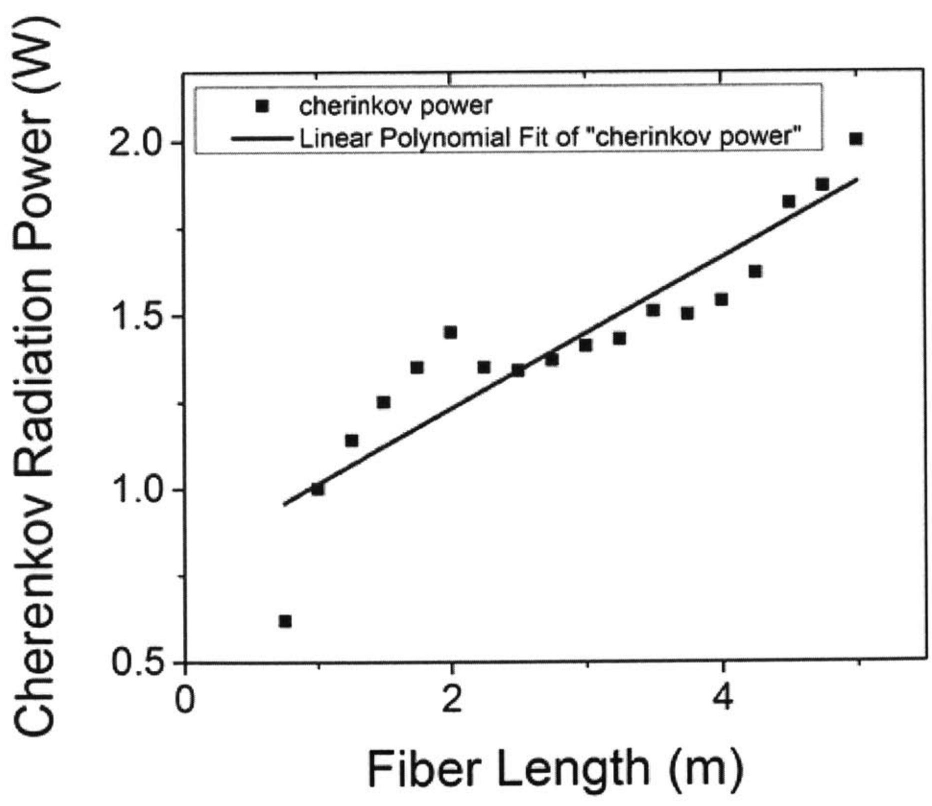

Fig.3.6. Output power of Cherenkov radiation with different fiber lengths.

Figure 3.5 shows the output power of the pulse after the LP02 positive fiber with different fiber lengths and a fixed incoming pump power. As is shown, when the fiber is long, the output power gets a little higher. However, when the fiber is less than 4 m, the output power is around 3W, relatively stablely. In Fig.3.6, however, the optical power of the filtered Cherenkov radiation decreases noticeably with decreasing LP02 positive fiber length, with a fixed incoming pump power. A fitting line of the points shows that the relation is almost linear.

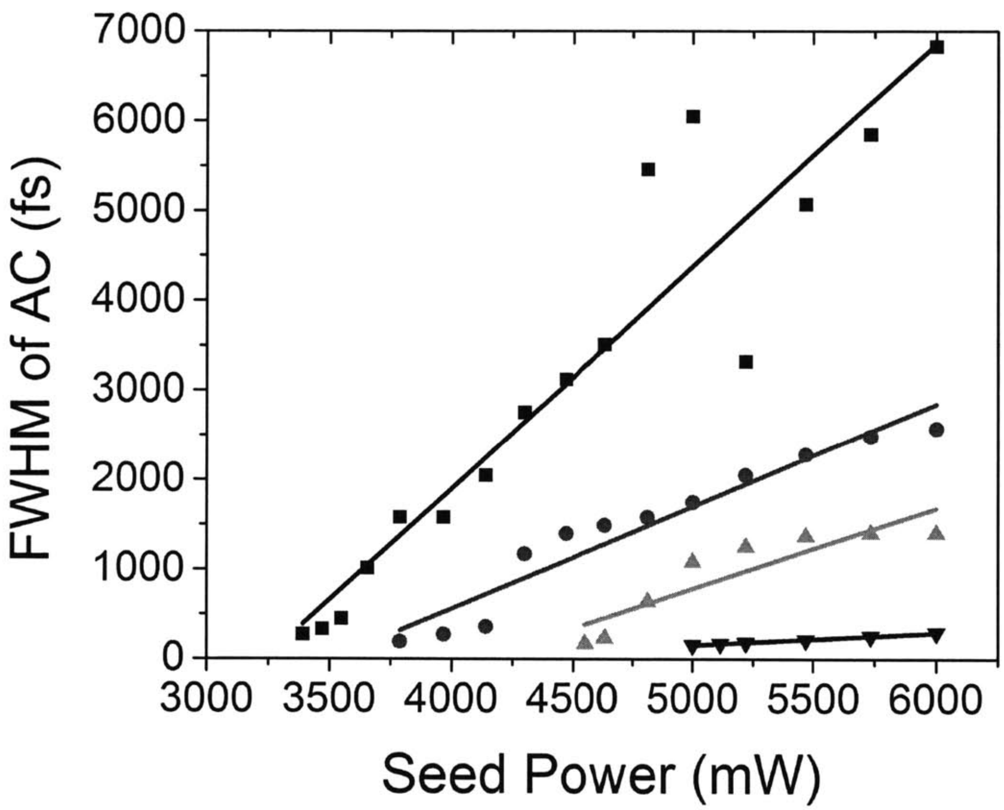

Fig.3.7. Pulse duration of the direct output Cherenkov radiation with different fiber length and different incoming pulse energy.

The maximum power we got is 3W with about 30% optical conversion efficiency when the fiber length is about 5 m and input power about 10W, but the fiber tip burned several times. By cutting back the fiber length, we achieved Cherenkov radiation with different output power and a fixed incoming power at 8W. This is due to the intrinsic characteristics of the mechanism of Cherenkov generation. The highest power in Fig.3.7 is 2 W when using 5 m fiber, whereas the output for 0.75 m fiber length is only around 0.6W. Similarly by cutting back and varying seed power at the same time, we measured the uncompressed pulse duration of the Cherenkov radiation (Fig.3.7). The black, red, green, and blue curves correspond to LP02 positive fiber with length of 2.75 m, 1.75 m, 1 m, and 0.75 m respectively. As the fiber length gets shorter, the Cherenkov radiation exhibits shorter pulse duration. When the fiber length is around 0.75 m, the autocorrelation trace of the uncompressed pulse duration is almost constant and has a FWHM around 200 fs. This optimal length is consistent with our simulation work mentioned before. However, when the fiber length is longer than the optimal length, the output pulse duration increases almost linearly with the input and output optical power. For 2.75 m long fiber, the pulse duration can be much longer.

This showed a trade-off: for the most output power of Cherenkov radiation, we need longer LP02 fiber. However, to get the minimum direct output pulse duration, the fiber length should be at the optimal length around 0.75m.

We are currently short of diffraction gratings with good efficiency to further compress the pulse at its highest power, partly due to the distorted shape of the output pulse when the fiber is long, and partly due to the poor degree of polarization of the output pulse.

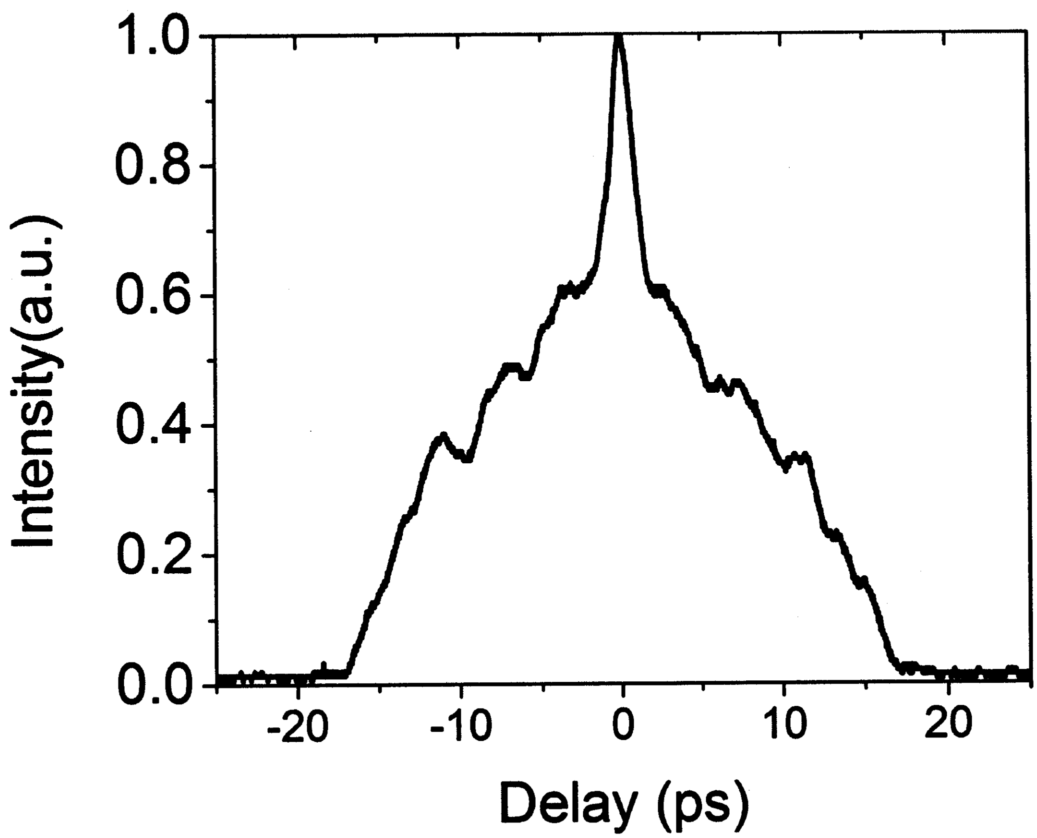

Fig.3.8. AC trace of direct output Cherenkov radiation with 5 m fiber.

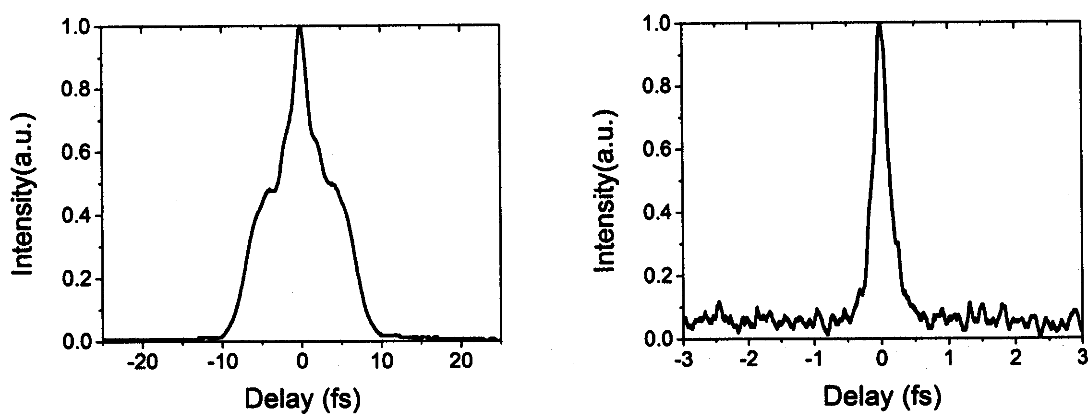

Fig.3.9. AC trace of direct output Cherenkov radiation with 2.75 m fiber and different incoming seed power: left: 3.2 W; right: 1.7 W.

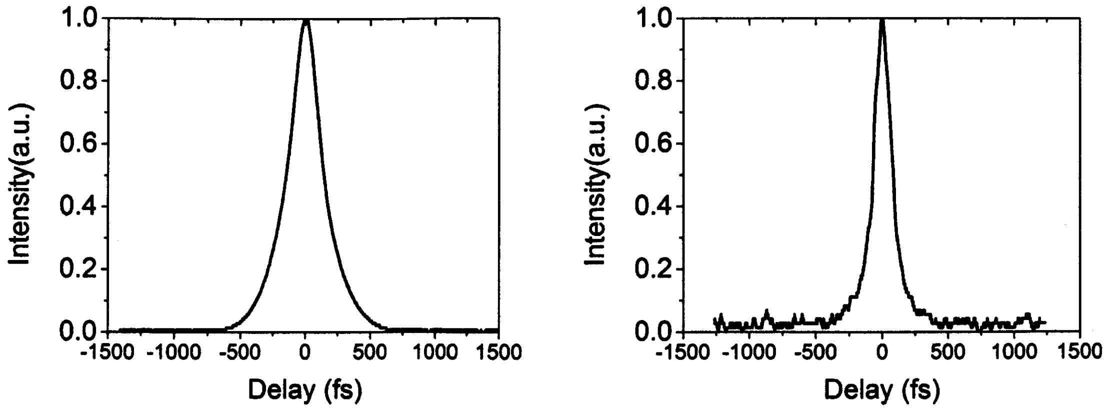

Fig.3.10. AC trace of direct output Cherenkov radiation with 0.75 m fiber and different incoming seed power: left: 3.0 W; right: 2.4 W.

Figure.3.8 shows the autocorrelation trace of the output Cherenkov radiation from a segment of 5 m LP02 positive fiber. The pulse is highly distorted due to the high peak power accumulated nonlinearity along the fiber. In Fig.3.9, it is clear that as the fiber was cut to 2.75 m, the pulse shape becomes much cleaner and shorter than the pulse duration with 5m LP02 fiber. As the fiber was cut further to 0.75 m in Fig.3.10, no pedestal appears in the autocorrelation trace. With 2.4 W incoming host pulses, the FWHM of the autocorrelation trace of the direct output Cherenkov radiation is only 155 fs.

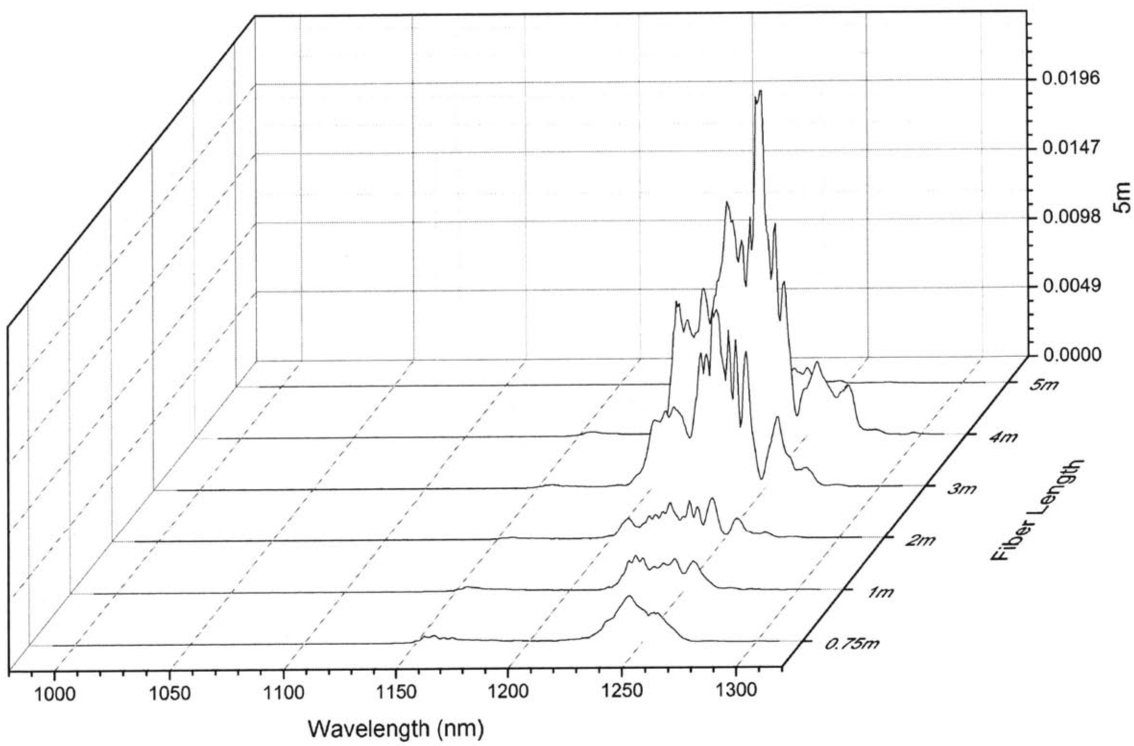

Fig.3.11. Spectra of output Cherenkov radiation with different fiber length.

Figure 3.11 shows the spectrum change with different fiber length with a fixed incoming seed power. The host pulse shifts more of its energy to the Cherenkov radiation pulses when the fiber length increases. To get the most in long wavelengths, the fiber should be long enough for the soliton to transfer energy.

3.3 Conclusion

We have demonstrated a system that can generate above 3 W average power of Cherenkov radiation by launching 3 GHz repetition rate femtosecond pulses into the LP02 positive fiber. The spectrum, conversion efficiency and direct output pulse duration change dramatically with the length of LP02 positive fiber. The shortest pulse duration of the output Cherenkov radiation is 155 fs with an average power about 0.6 W.

Conclusion and future work

In this thesis, we have demonstrated a novel way of generating optical pulses at 1018 nm with above 35 nJ pulse energy and 5 nm spectral bandwidth. Pulses can be compressed to the femtosecond regime. This laser system has a variety of applications particularly in seeding Yb:YLF regenerative amplifiers. We also developed a system that efficiently generated over 3W of Cherenkov radiation. The shortest Cherenkov pulse duration was 155 fs, which makes it a promising laser source for biomedical applications.

Future work of the 1018 nm laser system will be devoted to further increase the pulse energy while keep the compressibility. Simulation suggests that sub-microjoule pulse energy is possible if the pulse is stretched to 0.5 ns, which in turn either introduces tremendous third order dispersion if we use a fiber stretcher, or introduces the experimental implementation difficulty of using a diffraction grating pair as the stretcher.

Future work of the Cherenkov radiation will be focused on generating higher energy Cherenkov pulses and using transmission grating pair to compress them to under 500 fs. Simulation shows that over 5 nJ Cherenkov radiation is possible from this setup.

Appendix A

Implementation of the 1018 nm laser system

A.2 List of fiber components

Name	#	Description	specification
HI1060 fiber	20 m	Used for fiber pre-stretcher	
Yb1200-4/125 fiber	30 cm	Highly doped Yb fiber	Absorption: 1200 db/m@976 nm
1030 collimator	2 pieces	collimator	10 cm working distance, 0.03 dB Insertion loss
FWDM-9830-B-H-1-0-1W	1 piece	Filter WDM	Reflecting wavelength: 1020-1100nm
ISOS-30-B-1-0-0.08W	4 pieces	Polarization insensitive single stage isolator	1030 nm, Max IL: 4.0dB, Min isolation: 25dB
PBS	2 pieces	Polarization beam-splitter	
BPF	2 pieces	Bandpass filter	3.5 nm BW, 92% peak transmission
HWP	3 pieces	Half waveplate, for rotating the polarization of the beams	
QWP	2 pieces	Quarter waveplate, for transforming the elliptical polarization beam into linear polarization beam	
DCF-YB-	1 m	Yb-doped double-clad fiber	Absorption: 10.8

8/128P-FA		with flattened-top absorption	dB/m@976nm
MPC-2+1x1-105/125-10/125-70x12x8	1 piece	980/1030 beam combiner	Input Signal Fiber & Output Fiber: 10/125 DCF fiber, 0.08/0.46NA

Table.A.1 List of fiber components

A.2 Filter for 1018 nm

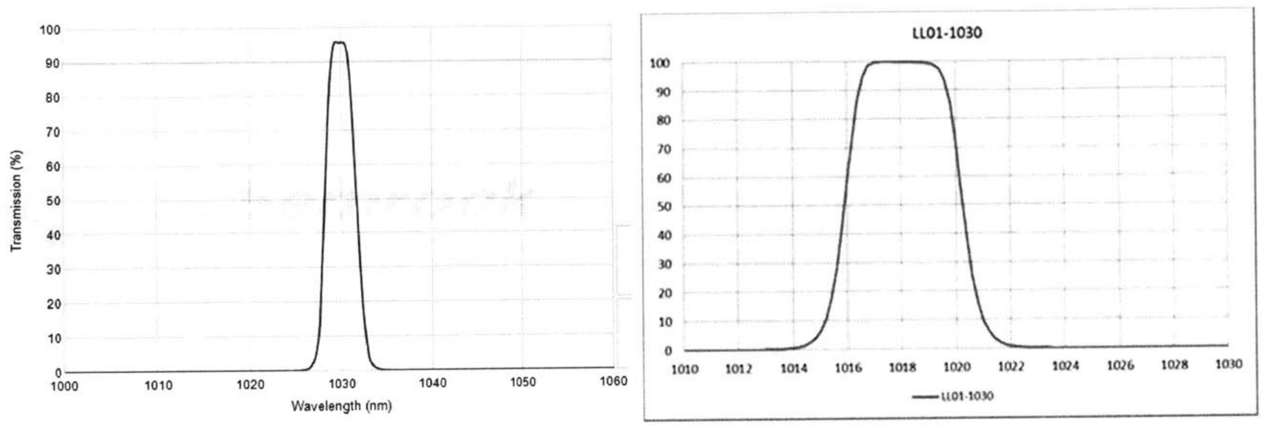

Fig.A.1. Transmission curve for the Maxline-1030 filter with normal incidence (left) and with angled incidence (right).

(source: www.semrock.com)

Formula (*) was used to calculate the center wavelength of the transmission curve when beam incidences with angle θ:

$$\lambda(\theta) = \lambda(0)\sqrt{1 - \frac{sin^2(\theta)}{n_{eff}^2}} \qquad (*)$$

Appendix B

Matlab simulation code for the 1018 nm oscillator

B.1. Introduction

This simulation model is already introduced in the previous section. The code was originally written in Fortran by Fatih Omer Ilday. A software with GUI can be downloaded at http://ultrafast.bilkent.edu.tr/UFOLAB/Home.html . Thanks to the development of Matlab Simulink library, we can wrap things up in a more compact and efficient way. Critical parameters for an oscillator simulation are: dispersion (k2, k3), saturation energy (Esat), gain bandwidth (g2), raman coefficient (Raman), output percentage (OC section), and modulation depth (NPR section).

B.2. Sample Code for the oscillator

Here we show a sample code for the simulation. This code can be adapted for simulating several kinds of fiber lasers (soliton-like/stretch-pulse/similariton mode-locked lasers), fiber amplifiers, fiber stretcher and diffraction grating compressors. Only the main code is provided. Some key functions are hidden. Contact the author if you want to know the detail.

Main code:

```
tres = 4096;        %%
Elast = zeros(tres,1);
Elast1 = zeros(tres,1);
criteria = zeros(5,1);

totalpasses = 1000;
saveevery = 10;

T0 = 4;
%%dz = 1.0/totalsteps;

for t = 1:tres
    Elast(t) = (1.665*T0+rand*t)/(tres+0.01);
end
%%%%%%%%%%%%%%%%%%%%%%%%%%%%%%%%%%%%
start = 0000;
conv = 1.665;
Treal = 100.0/conv;
Power = 1500.0;
Lambda = 1030.0;
Dtot = 0.0;
Ltot = 10.0;     %% free space length

%%redord the parameters.dat
%%%%%%%%%%%%%%%%%%%%%%%%%%%%%%%%%%%%
%%/****** set parameters ***********%%/
%%%%%%%%%%%%%%%%%%%%%%%%%%%%%%%%%%%%
L = [250.0, 20.0, 50.0]';
numEachSegment = [12, 40, 4]';
gain = [0.0001, 4.0, 0.0001]';
Esat = [1000.0, 3.0, 1000.0]'*T0; %% gain 30 db for small signal
g2 = [5000.0, 100.0, 5000.0]';    %% gain bandwidth
Raman = 5.0*T0/(Treal*1.0)*[1, 1, 1]';
k2 = [22.0, 22.0, 22.0]';
k3 = [74.0, 74.0, 74.0]';
n2 = [2.36, 2.36, 2.36]';
Aeff = [28.27, 15.20, 28.27]';
Gamma = 2.0*pi./Lambda.*n2./Aeff./10.0;
L2d = Treal.^2./k2./10.0;
L3d = Treal.^3./k3./10.0;
dz = 1./numEachSegment;
LnL = 1.0./(Power.*Gamma);
Lg = L./(1.15.*gain);
%%%%%%%%%%%%%%%%%%%%%%%%%%%%%%%%%%%%%%
Isat= 1.00;
Iglobal = 0.0;
%%%%%%%%%%%%%%%%%%%%%%%%%%%%%%%%%%%%%%
for pass = start+1:totalpasses
    sprintf('*******************\n Roundtrip = %d',pass);
    Iglobal = 0.0;
    Energy = sum(abs(Elast1).^2);
    Ipeak = max(abs(Elast1).^2);
    sprintf('Total energy out cavity is:  %.8f  pJ',
```

```
Energy*Power*Treal/(T0*1.0)/1000.0);
   %%%%%%%%%%%%%%%%%%%%%%%%%%%%%%%%%Converge Check
    criteria(mod(pass,5)+1) = Energy;
    disp(criteria');
    c= criteria;
    if ((c(5)-c(4))<1e-6*c(5) && (c(4)-c(3))<1e-6*c(4) && (c(3)-c(2))<1e-
6*c(3) && (c(2)-c(1))<1e-6*c(2))
          disp('The field has converged!!!');
          fid = fopen('Converged.dat','w');
          for t = 1:tres
             Ereal = real(Elast1(t));
             Eimag = imag(Elast1(t));
             Phi = -atan2(Eimag, Ereal);
             fprintf(fid,'%.8f %.8f %.8f \r\n', t, Ereal, Eimag);
          end
          fid = fclose(fid);
        break;
    end
%%Go through each segment of fiber/components
    for i = 1:3
        for stepNum = 1:numEachSegment(i)
            Elast = Propagate(Elast, dz(i), L(i), L2d(i), L3d(i), LnL(i),
Lg(i), Esat(i), g2(i), Raman(i));
            Ipeak = max(abs(Elast).^2);
            Iglobal = max(Iglobal, Ipeak);
            Energy = sum(abs(Elast).^2);
        end
    end

    sprintf('Overall peak Power is  %.6f  W', Iglobal*Power);

%% Saturable Absorber action
    Icenter= Ipeak;
    Elast1 = Elast;
    Elast = Elast.*sqrt(1.0 - 0.7./(1+abs(Elast).^2/Isat));
    Elast1 = Elast1 - Elast;

%% Output Coupler action
    Elast = Elast*sqrt(0.3);
%% filter Coupler action
    fact = 50;              %%4096/100/10 = 4 nm
    factor = (1:tres)';
    factor = exp(fact*(factor-tres/2).^2/tres^2)/exp(fact/4);
    Elast = ifft(fft(Elast,tres).*factor, tres);
end %%/end all passes
```

Table.A.2 Sample of simulation code

Bibliography

[1] R. L. Fork, O. E. Martinez, and J. P. Gordon, “Negative dispersion using pairs of prisms,” Opt. Lett. 9, 150-152.

[2] E. B. Treacy, “Optical pulse compression with diffraction gratings,” IEEE J. Quantum Electron. QE-5, 454-458(1969).

[3] R. Szipocs, K. Ferencz, C. Spielmann, and F. Krausz, “Chirped multilayer coatings for broadband dispersion control in femtosecond lasers,” Opt. Lett. 19, 201-203 (1994).

[4] H. Lim, F. Ilday, and F. Wise, “Femtosecond ytterbium fiber laser with photonic crystal fiber for dispersion control,” Opt. Express 10(25), 1497–1502 (2002).

[5] H. Lim and F. Wise, “Control of dispersion in a femtosecond ytterbium laser by use of hollow-core photonic bandgap fiber,” Opt. Express 12(10), 2231–2235 (2004).

[6] A. Isomäki and O. G. Okhotnikov, “Femtosecond soliton mode-locked laser based on ytterbium-doped photonic bandgap fiber,” Opt. Express 14(20), 9238–9243 (2006).

[7] F. O. Ilday, J. R. Buckley, H. Lim, F. W. Wise, and W. G. Clark, “Generation of 50-fs, 5-nJ pulses at 1.03 μm from a wave-breaking-free fiber laser,” Opt. Lett. 28, 1365-1367 (2003).

[8] Andy Chong, Joel Buckley, Will Renninger, and Frank Wise, "All-normal-dispersion femtosecond fiber laser," Opt. Express 14, 10095-10100 (2006).

[9] Andy Chong, William H. Renninger, and Frank W. Wise, "Properties of normal-dispersion femtosecond fiber lasers," J. Opt. Soc. Am. B 25, 140-148 (2008).

[10] P. K. A. Wai, C. R. Menyuk, Y. C. Lee, and H. H. Chen, “Nonlinear pulse propagation in the neighborhood of the zero-dispersion wavelength of monomode optical fibers,” Opt. Lett. 11(7), 464–466 (1986).

[11] P. K. A. Wai, H. H. Chen, and Y. C. Lee, “Radiations by “solitons” at the zero group-dispersion wavelength of single-mode optical fibers,” Phys. Rev. A 41(1), 426–439 (1990).

[12] V. I. Karpman, “Radiation by solitons due to higher-order dispersion,” Phys. Rev. E

Stat. Phys. Plasmas Fluids Relat. Interdiscip. Topics 47(3), 2073–2082 (1993).

[13] N. Akhmediev and M. Karlsson, "Cherenkov radiation emitted by solitons in optical fibers," Phys. Rev. A 51(3), 2602–2607 (1995).

[14] J. N. Elgin, T. Brabec, and S. M. J. Kelly, "A perturbative theory of soliton propagation in the presence of third order dispersion," Opt. Commun. 114(3–4), 321–328 (1995).

[15] A. V. Husakou and J. Herrmann, "Supercontinuum generation of higher-order solitons by fission in photonic crystal fibers," Phys. Rev. Lett. 87, 203901 (2001).

[16] L. Tartara, I. Cristiani, and V. Degiorgio, "Blue light and infrared continuum generation by soliton fission in a microstructured fiber," Appl. Phys. B 77, 307 (2003).

[17] G. Genty, M. Lehtonen, and H. Ludvigsen, "Effect of cross-phase modulation on supercontinuum generation in microstructured fibers with sub-30 fs pulses," Opt. Express 12, 4616 (2004).

[18] D. R. Austin, C. Martijn de Sterke, B. J. Eggleton, and T. G. Brown, "Dispersive wave blue-shift in supercontinuum generation," Opt. Express 14, 11997 (2006).

[19] A. V. Gorbach and D. V. Skryabin, "Light trapping in gravity-like potentials and expansion of supercontinuum spectra in photonic-crystal fibres," Nature Photonics 1, 653 (2007).

[20] S. P. Stark, A. Podlipensky, N. Y. Joly, and P. St. J. Russell, "Ultraviolet-enhanced supercontinuum generation in tapered photonic crystal fiber," J. Opt. Soc. Am. B. 27, 592 (2010).

[21] A. V. Mitrofanov, Y. M. Linik, R. Buczynski, D. Pysz, D. Lorenc, I. Bugar, A. A. Ivanov, M. V. Alfimov, A. B. Fedotov, and A. M. Zheltikov, "Highly birefringent silicate glass photonic-crystal fiber with polarization-controlled frequency-shifted output: A promising fiber light source for nonlinear Raman microspectroscopy," Opt. Express 14, 10645 (2006).

[22] H. Tu and S. A. Boppart, "Optical frequency up-conversion by supercontinuum-free widely-tunable fiber-optic Cherenkov radiation," Opt. Express 17, 9858 (2009).

[23] H. Tu and S. A. Boppart, "Ultraviolet-visible non-supercontinuum ultrafast source enabled by switching single silicon strand-like photonic crystal fibers," Opt. Express 17, 17983 (2009).

[24] D. V. Skryabin, F. Luan, J. C. Knight, and P. S. Russell, "Soliton self-frequency shift cancellation in photonic crystal fibers," Science 301, 1705-1708 (2003).

[25] I. Cristiani, R. Tediosi, L. Tartara, and V. Degiorgio, "Dispersive wave generation by solitons in microstructured optical fiber," Opt. Express 12, 124-135 (2004).

[26] F. Lu and W. H. Knox, "Generation, characterization, and application of broadband coherent femtosecond visible pulses in dispersion micromanaged holey fibers," J. Opt. Soc. Am. B 23, 1221-1227 (2006).

[27] Guoqing Chang, Li-Jin Chen, and Franz X. Kärtner, "Fiber-optic Cherenkov radiation in the few-cycle regime," Opt. Express 19, 6635-6647 (2011).

[28] James van Howe, Jennifer H. Lee, Shian Zhou, Frank Wise, Chris Xu, Siddharth Ramachandran, Samir Ghalmi, and Man F. Yan, "Demonstration of soliton self-frequency shift below 1300nm in higher-order mode, solid silica-based fiber," Opt. Lett. 32, 340-342 (2007).

[29] J. H. Lee, J. van Howe, C. Xu, S. Ramachandran, S. Ghalmi, and M. F. Yan, " Generation of Femtosecond Pulses at 1350 nm by Cherenkov Radiation in Higher-Order-Mode Fiber," in Optical Fiber Communication Conference and Exposition and The National Fiber Optic Engineers Conference, OSA Technical Digest Series (CD) (Optical Society of America, 2007), paper OThO3.

[30] N. Coluccelli, G. Galzerano, L. Bonelli, A. Di Lieto, M. Tonelli, and P. Laporta, "Diode-pumped passively mode-locked Yb:YLF laser," Optics Express, Vol. 16, Issue 5, pp. 2922-2927 (2008).

[31] Junji Kawanaka, Koichi Yamakawa, Hajime Nishioka, Ken-ichi Ueda, "30-mJ, diode-pumped, chirped-pulse Yb:YLF regenerative amplifier," Optics Letters, Vol. 28, Issue 21, pp. 2121-2123 (2003).

[32] Jianhua Wang, Gui Chen, Lei Zhang, Jinmeng Hu, Jinyan Li, Bing He, Jinbao Chen, Xijia Gu, Jun Zhou, and Yan Feng, "High-efficiency fiber laser at 1018 nm using Yb-doped phosphosilicate fiber," Applied Optics, Vol. 51, Issue 29, pp. 7130-7133 (2012).

[33] Hu Xiao, Pu Zhou, Xiaolin Wang, Shaofeng Guo and Xiaojun Xu, "Experimental Investigation on 1018-nm High-Power Ytterbium-Doped Fiber Amplifier," Photonics Technology Letters, IEEE, Vol 24, Issue 13, pp.1088-1090(2012).

[34] J. Buckley, F. O. Ilday, H. Lim, F. W. Wise, "Self-similar pulses as a route to low-repetition-rate femtosecond fiber lasers", Lasers and Electro-Optics, 2004. (CLEO).

Conference, CTHK7.

[35] W. H. Renninger, A. Chong, and F. W. Wise, "Giant-chirp oscillators for short-pulse fiber amplifiers," Opt. Lett. 33, 3025-3027 (2008).

[36] S. Zhou, D. G. Ouzounov, C. Sinclair, and F. W. Wise, "Generation of 400-fs solitons with 2-MHz repetition rate by a Yb-fiber laser," Lasers and Electro-Optics Society, LEOS 2006, 19th Annual Meeting of the IEEE, 209-210 (2006).

[37] Lih-Mei Yang, Peng Wan, Vladimir Protopopov, and Jian Liu, "2 μm femtosecond fiber laser at low repetition rate and high pulse energy," Opt. Express 20, 5683-5688 (2012).

[38] Omid Nohadani, Jonathan R. Birge, Franz X. Kärtner, and Dimitris J. Bertsimas, "Robust chirped mirrors," Appl. Opt. 47, 2630-2636 (2008).

[39] Sergey Kobtsev, Sergey Kukarin, and Yurii Fedotov, "Ultra-low repetition rate mode-locked fiber laser with high-energy pulses," Opt. Express 16, 21936-21941 (2008).

[40] Kong, L.J., Xiao, X.S. and Yang, C.X. (2010), Low-repetition-rate all-fiber all-normal-dispersion Yb-doped mode-locked fiber laser. Laser Phys. Lett., 7: 359–362.

[41] D. Mortag, J. Neumann, D. Kracht, U. Morgner, D. Wandt, H. Sayinc, "93 fs pulses from a low repetition rate fiber laser", IEEE, Lasers and Electro-Optics 2009 and the European Quantum Electronics Conference, 1, 2009.

[42] S. V. Marchese, C. R. Baer, A. G. Engqvist, S. Hashimoto, D. J. Maas, M. Golling, T. Südmeyer, and U. Keller, "Femtosecond thin disk laser oscillator with pulse energy beyond the 10-microjoule level," Opt. Express 16, 6397-6407 (2008).

[43] H Sayinc, D. Mortag, D. Wandt, J. Neumann, and D. Kracht, "Sub-100 fs pulses from a low repetition rate Yb-doped fiber laser," Opt. Express 17, 5731-5735 (2009).

[44] William H. Renninger, Andy Chong, and Frank W. Wise, "Pulse Shaping and Evolution in Normal-Dispersion Mode-Locked Fiber Lasers", Selected Topics in Quantum Electronics, IEEE Journal of, Vol.18, Iss. 1, 389-398(2012).

[45] Bulent Oktem, Coşkun Ülgüdür, and F. Ömer Ilday, "Soliton–similariton fibre laser", Nature Photonics 4, 307 - 311 (2010).

[46] Yury Logvin, V. P. Kalosha, and Hanan Anis, "Third-order dispersion impact on mode-locking regimes of Yb-doped fiber laser with photonic bandgap fiber for dispersion compensation," Opt. Express 15, 985-991 (2007).

[47] K. S. Kim, W. A. Reed, K. W. Quoi, and R. H. Stolen, "Measurement of the nonlinear index of silica-core and dispersion-shifted fibers," Opt. Lett. 19, 257-259 (1994).

[48] Alistair Gorman, David William Fletcher-Holmes, and Andrew Robert Harvey, "Generalization of the Lyot filter and its application to snapshot spectral imaging," Opt. Express 18, 5602-5608 (2010).

[49] Andy Chong, William H. Renninger, and Frank W. Wise, "Route to the minimum pulse duration in normal-dispersion fiber lasers," Opt. Lett. 33, 2638-2640 (2008).

[50] N. Nishizawa and T. Goto, "Experimental analysis of ultrashort pulse propagation in optical fibers around zerodispersion region using cross-correlation frequency resolved optical gating," IEEE Photon. Technol. Lett. 11, 325 (1999).

[51] M. E. Fermann, A. Galvanauskas, M. L. Stock, K. K. Wong, D. Harter, and L. Goldberg, "Ultrawide tunable Er soliton fiber laser amplified in Yb-doped fiber," Opt. Lett. 24, 1428-1430 (1999).

[52] X. Liu, C. Xu, W. H. Knox, J. K. Chandalia, B. J. Eggleton, S. G. Kosinski, and R. S. Windeler, "Soliton self-frequency shift in a short tapered air–silica microstructure fiber," Opt. Lett. 26, 358-360 (2001).

[53] B. R. Washburn, S. E. Ralph, P. A. Lacourt, J. M. Dudley, W. T. Rhodes, R. S. Windeler, and S. Coen, "Tunable near-infrared femtosecond soliton generation in photonic crystal fibres," Electron. Lett. 37, 1510 (2001).

[54] H. Lim, J. Buckley, A. Chong, and F. W. Wise, "Fibre-based source of femtosecond pulses tunable from 1.0 to 1.3 um," Electron. Lett. 40, 1523 (2004).

[55] F. Luan, J. Knight, P. Russell, S. Campbell, D. Xiao, D. Reid, B. Mangan, D. Williams, and P. Roberts, "Femtosecond soliton pulse delivery at 800nm wavelength in hollow-core photonic bandgap fibers," Opt. Express 12, 835-840 (2004).

[56] S. Ramachandran, S. Ghalmi, J. W. Nicholson, M. F. Yan, P. Wisk, E. Monberg, and F. V. Dimarcello, "Anomalous dispersion in a solid, silica-based fiber," Opt. Lett. 31, 2532-2534 (2006).

[57] Hung-Wen Chen, Guoqing Chang, Shanhui Xu, Zhongmin Yang, and Franz X. Kärtner, "3 GHz, fundamentally mode-locked, femtosecond Yb-fiber laser," Opt. Lett. 37, 3522-3524 (2012).